ORIGINAL PAPER



"Drive-by" bridge frequency-based monitoring utilizing wavelet transform

Chengjun Tan¹ • Ahmed Elhattab¹ • Nasim Uddin¹

Received: 6 June 2017/Accepted: 6 October 2017/Published online: 23 October 2017 © Springer-Verlag GmbH Germany 2017

Abstract In recent years, the concept of bridge monitoring using indirect measurements from a passing vehicle has been rapidly developed. This concept is known as "driveby bridge inspection". Most of the methods proposed under this approach utilize the dynamic characteristics of the bridge as an indicator of damage, such as the natural frequency of the bridge. The natural frequency is often estimated using fast Fourier transform (FFT). However, FFT has a low frequency resolution at the condition of higher velocity of a passing vehicle; therefore, it is not appropriate to be used to monitor the frequency change caused by the degradation of the bridge structural integrity. This paper introduces a new frequency identification technique based on wavelet analysis. Wavelet transform is characterized by its high-frequency resolution and can, therefore, be used to visualize the bridge damage represented as changing the fundamental frequency of the bridge. The paper will implement this approach using an implicit Vehicle-Bridge Interaction (VBI) algorithm to simulate the passage of the inspection vehicle over the bridge. The acceleration signals are then processed using wavelet analysis to extract the bridge frequency. In addition, the study will investigate the use of a subtracted signal from two consecutive axles. The latter point has the advantage of substantially removing the effect of the road roughness from the recorded acceleration history.

Keywords Wavelet transform · Wavelet pseudofrequency · Bridge damage detection · Drive-by bridge inspection · Structural health monitoring

1 Introduction

The structural integrity of bridges, as the main component of transport infrastructure, is an integral part of the safety of transport facilities. However, bridges are subject to continuous degradation due to environmental impacts and an excessive increase in the weight of traffic over time. Therefore, bridge structures require continuous monitoring to ensure maintenance and hence their structural integrity. Traditionally, visual inspection is regarded as one of the most common methods to inspect bridges; however, it only provides a qualitative measure of the bridge health index [1]. In addition, the human factor reduces the credibility of the method wherein a number of bridges collapsed catastrophically, whereas they had been visually inspected just before the disaster. Thus, Chupanit and Phromsorn [2] have suggested that visual inspection alone may not be sufficient to monitor the structural health of the bridges. Recently, Structural Health Monitoring (SHM) technologies, which rely on automatic detection of anomalous structural behavior, have evolved dramatically. There are four distinguishing levels of SHM [3, 4]: (1) identify whether the damage exists, (2) locate the damage, (3) determine the damage level and (4) calculate the remaining service life of the structure. Conventional SHM methods require a large number of sensors on the structure [4]. This approach is expensive, time-consuming, and even dangerous, limiting

Ahmed Elhattab aahattab@uab.edu

Nasim Uddin nuddin@uab.edu



[☐] Chengjun Tan tan1990@uab.edu

The University of Alabama at Birmingham, 1075 13th St S, Birmingham, AL 35205, USA

the expansion of the approach to a large number of bridges [1]. From another perspective, short and medium span bridges represent a large portion of the bridge inventory of the road network, and conventional bridge health monitoring could not be used for the aforementioned drawbacks. From another perspective, a large number of medium to short bridges operate for several years, requiring an assessment of their current structural health condition, while this cannot be achieved using traditional monitoring techniques due to the aforementioned obstacles [1]. Thus, there is a necessity to find a less expensive SHM method that could be applied to a broad number of bridges.

The idea of an indirect approach, or what has been known as 'drive-by bridge inspection', is based on extracting the dynamic properties of the bridge structures from the dynamic response of a passing vehicle over the bridge, which was first proposed by Yang et al. [5, 6]. The authors adopted a fast Fourier transform (FFT) to find the bridge frequency from the dynamic response of a passing vehicle. It is shown that the vehicle response is dominated by four specific frequencies: the vehicle frequency, driving frequency of the moving vehicle and two shifted frequencies of the bridge. The feasibility of such indirect method in practice has been experimentally verified by Yang and Chang [7] and Lin and Yang [8] via passing an instrumented vehicle over a bridge. Yang et al. [9] constructed bridge modal shapes successfully from a passing vehicle by employing Hilbert Transform combined with band-filter technical, and pointed out that the indirect measurements from the inspection vehicle, give a better screening for the bridge degrees of freedom than the direct measurements from an installed sensor on the bridge structure.

Yang and Chang [7] decomposed acceleration history of a passing instrumented vehicle with the empirical mode decomposition (EMD) to generate the intrinsic mode functions (IMFs). Then generated IMFs were adopted by FFT to successfully extract bridge natural frequencies of higher modes, instead of the original recorded response. Lin and Yang [8] used a two-wheel cart towed by a light truck to extract the fundamental frequency of the bridge. In this truck-cart system, truck acts as an exciter for the bridge, while accelerometers are installed in the cart making it function as a receiver for bridge responses. It has been proven that the bridge frequencies can be successfully deduced from the acceleration histories of the cart utilizing FFT.

Since the concept of the drive-by bridge inspection emerged, many studies have been conducted to investigate the limits of the approach [7, 8, 10–15]. Yang et al. [5] showed that higher speeds provide higher visibility of the bridge frequency in the vehicle's acceleration spectrum. This study has been carried out assuming a smooth road profile. By contrast, recent research has revealed that when road roughness is taken into account, vehicle responses dominate

the acceleration spectrum, and the bridge frequency cannot be extracted in this case [10]. Therefore, Lin and Yang [8], Fujino et al. [16] pointed out that lower vehicle speeds provides the best accuracy for estimating the bridge frequency, due to higher spectral resolution and the smaller impact of the road surface profile on the vehicle responses.

Wavelet transform is a robust signal-processing tool, characterized by its sensitivity to the discontinuities in the signal. Therefore, it has the ability to localize bridge damage. Khorram et al. [17] employed a wavelet based damage detection approach to estimate the location of damage in a numerical simulation beam subjected to a moving force. They use a moving sensor that calculates the displacement under the passing load. Using the sensor readings they computed the Continuous Wavelet Transform (CWT). The results revealed that highest magnitude of a CWT coefficient occurred at the exact location of the crack. The value of the highest magnitude of the CWT is directly correlated to the extent of the damage, and hence it can be considered an indicator of damage. Moreover, the study found that the moving sensor is superior to the fixed sensor, in terms of localization of damage. In another application of wavelet transformations in the localization of damage, Poudel et al. [18], Shahsavari et al. [19] have theoretically localized structural damage in the bridge by employing the wavelet transform with mode shape difference function.

Nguyen and Tran [20] introduced multi-cracks detection in the bridge structure based on wavelet transform, using theoretical VBI model. A moving vehicle will observe small distortions in the vibration responses at the crack locations. The authors used the wavelet transform to effectively find these small distortions so as to identify the crack location. McGetrick and Kim [21] employed the wavelet transforms to identify and localize the bridge damage, by harnessing a passing vehicle responses. The approach has been explored using theoretical VBI model and utilizing scaled laboratory test. The effect of bridge span length, vehicle mass, vehicle velocity, damage size or level to road surface roughness on the accuracy of results were investigated.

In this study, wavelet transform is applied to vehicle responses to detect the drop in the bridge natural frequency due to structural damage. The drop of the natural frequency will be used as an index to reflect the extent of the bridge damage. The study will be carried out using an implicit VBI algorithm to simulate the passage of the inspection vehicle over the bridge. The vehicle accelerations are recorded and analyzed to quantify the drop in the bridge frequency due to damage, if exist. In addition, the study will investigate the use of a subtracted signal from a two consecutive axles to extract the bridge frequency in order to substantially remove the effect of the road roughness from the recorded acceleration history.



2 Wavelet theory

In 1982. Jean Morlet coined the idea of the wavelet transform [22]. Mathematically, the idea behind wavelet analysis is to express or to approximate a signal or function by a family of functions constructed from dilatations and translations of a single function called the base wavelet [23, 24]. Hence, wavelet transform is similar to the Fourier transform (FT) that uses a series of cosine functions to approximate the objective signal. When applying FT to a signal, it defines the different frequencies contained by the signal with no clue about the time domain properties of the signal. In other words, FT only works as a signal-converting tool from time domain to frequency domain. On the other hand, wavelet method transforms the signal into time-frequency domain. This means that, performing wavelet transforms, a signal is shown in the frequency domain while retaining the time domain characteristics of the signal. Thus, the approach has a strong potential to identify localized change in bridge properties from a short data recorded from a passing vehicle.

2.1 Continuous wavelet transform

The continuous wavelet transform is defined as follows:

$$WT(a,b) = \int_{-\infty}^{+\infty} f(t) \frac{1}{\sqrt{a}} \Psi\left(\frac{t-a}{a}\right) dt \quad a \in \mathbb{R}^+, \ b \in \mathbb{R},$$
(1)

where WT(a,b) is the complex wavelet coefficients or wavelet transform; a and b are real scale and translation-parameters. $\Psi_{a,b}(t)$ denotes the conjugate of the complex mother wavelet function which satisfies the properties of $\int\limits_{-\infty}^{+\infty} \Psi(t) \mathrm{d}t = 0$ and $\int\limits_{-\infty}^{+\infty} |\Psi(t) \mathrm{d}t| < \infty$. For example, Mexican hat ('Mexh') wavelet as shown in Fig. 1 is one of the

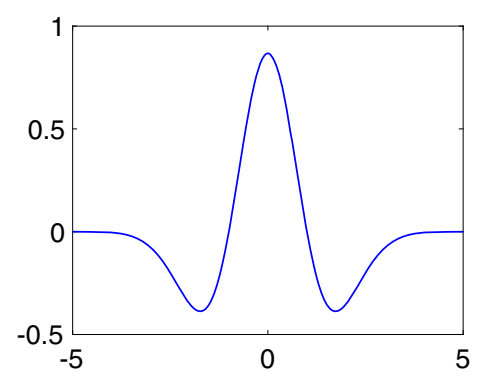


Fig. 1 Mexican hat wavelet functions

most popular mother wavelet functions and its mathematical expression is:

$$\Psi(t) = (1 - t^2)e^{\frac{-t^2}{2}},\tag{2}$$

when continuous wavelet transform is applied to the objective signal, it returns a series of wavelet coefficients at each scale in the time domain. The scales are correlated to the signal frequencies. A high value for the scale implies having a stretched wavelet, and hence a low-frequency content. In contrast, a low value for the scale implies having a high-frequency content. The mathematical relationship between scale and frequency is defined as follows:

$$F_{\rm S} = \frac{F_{\rm C}}{a\Lambda},\tag{3}$$

where $F_{\rm S}$ is a pseudo-frequency that corresponds to scale a in Hz, $F_{\rm C}$ is the central frequency of the wavelet in Hz (central frequency refers to the frequency of a periodic signal that most closely resembles the wavelet), a is the scale of the wavelet, and Δ is the sampling period of the signal. For the Mexican hat wavelet, $F_{\rm C}=0.25$ Hz.

2.2 Wavelet energy coefficient

The energy content of the signal is a unique measure for the signal. Similarly, the energy content of a signal can be calculated from its wavelet coefficients and its mathematical expression is:

$$E_{\text{energy}} = \sum_{a} \sum_{b} |WT(a, b)|^2. \tag{4}$$

Equation 4 indicates that the energy associated with each particular scaling parameter *a* is expressed as:

$$E_{\text{energy}} = \sum_{b}^{N} |WT(a,b)|^{2}, \tag{5}$$

where N is the number of wavelet coefficients, and WT(a,b) represents the wavelet coefficients at scale a.

For the objective signal, if a major frequency component corresponding to a particular scale 's' exists, then its wavelet energy coefficients at that scale will have relatively high magnitudes at the time when this major frequency component occurs [25]. As a result, the energy plot will point out to the dominating frequencies in the signal. This is why the wavelet analysis could be used to extract the bridge frequency from the dynamic response of a passing vehicle, where the frequency components at the bridge frequencies are expected to show a high energy magnitude in the scale plot.



3 Extracting bridge frequency from numerical VBI model

3.1 Vehicle bridge interaction (VBI) modeling

This section describes the VBI model employed to simulate the response of the bridge structure under the moving vehicle. The road surface profile is not considered in this simulation. At first, the vehicle is modeled as a quarter-car model crossing a 20-m approach distance followed by a 15-m simply supported finite element (FE) bridge (Fig. 2). The quarter-car travels with constant speed. The vehicle masses are represented by a sprung mass, m_s , and unsprung mass, m_a represents the vehicle axle mass and body mass, respectively. The degrees of freedoms (DOFs) that correspond to the bouncing of the sprung and the axle masses are, u_s , and u_a , respectively. The properties of the quarter-car and the bridge are listed in Table 1 and based upon the work of Cebon [26] and Harris et al. [27]. The dynamic interaction between the vehicle and the bridge is implemented in MATLAB [28, 29]. Unless otherwise mentioned, the used scanning frequency is 1000 Hz. The first natural frequency of bridge, f_b is 3.86 Hz. The vehicle frequencies are 0.58 and 8.65 Hz, respectively.

3.2 Identifying bridge frequency using the vehicle responses

Figure 3 illustrates the vehicle axle acceleration response for the VBI model mentioned above, where the vehicle velocity is 2 m/s. The x-axis shows the normalized position of the vehicle axle on the bridge with respect to the bridge length (L) (0 and 1 when the axle is at the start and at the end of the bridge, respectively). Yang et al. [5, 6] have proved that the acceleration history of a crossing vehicle over a bridge contains the bridge frequency components; therefore, the bridge frequency could be extracted after applying FFT to the signal. Figure 4b illustrates the spectrum of the recorded acceleration showing a distinctive peak associated with the fundamental frequency of the bridge (3.87 Hz). In addition, the spectrum of Fig. 4a

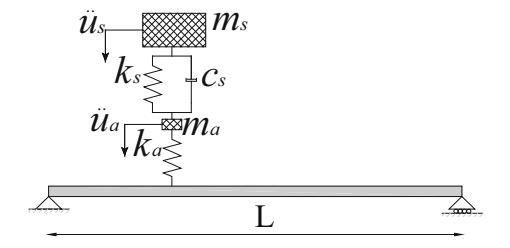


Fig. 2 The quarter-car and bridge model



Table 1 Vehicle and bridge properties

Vehicle properties		Bridge prope	Bridge properties	
$m_{\rm s}$	14,000 kg	Span	15 m	
$k_{\rm s}$	200 kN/m	Density	4800 kg/m^3	
$c_{\rm s}$	10 kN s/m	Width	4 m	
$m_{\rm a}$	1000 kg	Depth	0.8 m	
$k_{\rm a}$	2750 kN/m	Modulus	$2.75 \times 10^{10} \text{ N/m}^2$	

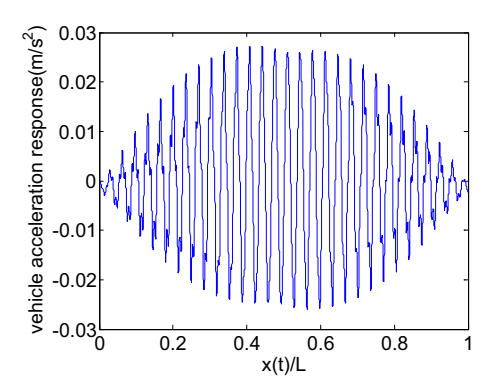


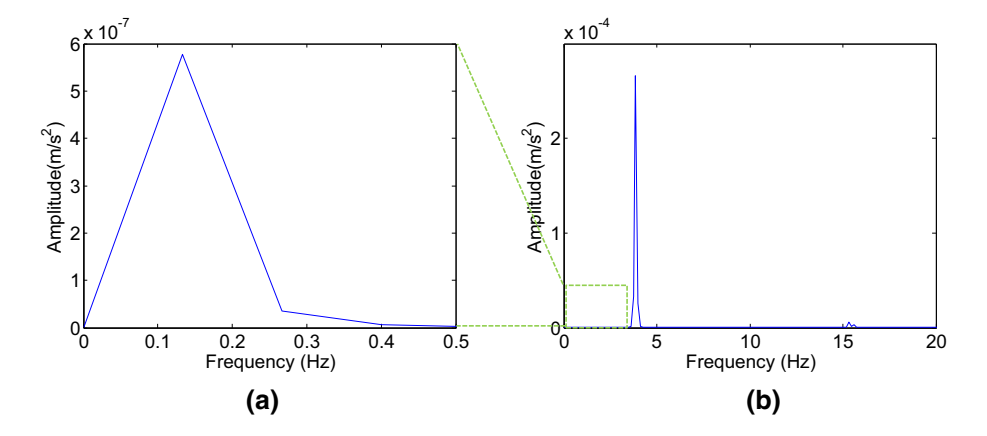
Fig. 3 The vehicle acceleration response

shows the driving frequency extracted as 0.13 Hz (the theoretical driving frequency = v/L = 0.13 Hz).

The 'Mexican hat' mother wavelet function is used to employ wavelet transform to the vehicle signal, and then the 'scaleogram' is plotted as shown in Fig. 5. This 'scaleogram' is a visual representation that displays the result from wavelet transforms, which is equivalent to the spectrogram for wavelets. There are three axes: two mutually perpendicular axes with relative distance in horizontal axis and wavelet coefficient 'a' on the vertical axis, and 'z' represents the values of the relative energy 'E', which is expressed in the plot using colors. Figure 5, shows a local increase in the absolute value of the wavelet coefficients between a = 30 and a = 110, with a dominating peak at approximately a = 65.

Equation 5 is used to compute the energy of every scale 'a'. The wavelet energy coefficient distribution at each scale, varying from 1 to 4000 with 0.1 increments is shown in Fig. 6a. This figure shows a sharp and a gentle peak in wavelet coefficient. Figure 6b shows this sharp increase between a=30 and a=110 as previously noted in Fig. 5. The peak after smoothing is found at a=65.4 (Fig. 6c). The pseudo-frequency corresponding to a=65.4 is calculated using Eq. 3 and found to be 3.82 Hz, which is close to the bridge frequency (3.86 Hz). Similarly, the peak of the gentle increase is found at a=1860 corresponding to frequency of 0.13 Hz, which is represented by the driving frequency.

Fig. 4 Acceleration spectrum of vehicle acceleration history, a frequency from 0 to 0.5 Hz, b frequency from 0 to 20 Hz



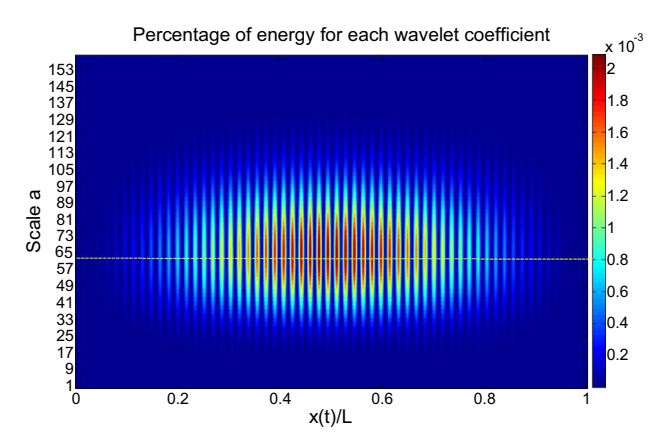


Fig. 5 Percentage of energy for each wavelet coefficient

There are a large number of commonly used mother wavelet functions. When applying different mother functions on the same objective signal, the results may changes. In this paper, it has been found that not all of these base mother wavelet functions could be used to accurately identify the natural frequency of the bridge. Only can Mexican hat and 'bior2.2' etc. provide the highest accuracy in extracting the bridge frequency from the vehicle responses. In this study, the Mexican hat wavelet will be used in the analysis of the acceleration signal, unless otherwise mentioned.

Herein, the study will investigate the efficacy of the Wavelet Transform in extracting the bridge frequency for different speeds. In this part, different velocities (4, 6, 8 and 10 m/s) are investigated. All other VBI model parameters are kept the same. Utilizing the techniques discussed above, the bridge frequency is extracted for every speed using Wavelet Transform. The results are listed in Table 2. The identified bridge frequency based on wavelet transforms corresponds to a particular scale that has the highest energy.

From Table 2, it is obvious that wavelet transform can give precise results (error less than 1.36%). The increase of

vehicle velocity leads to the driving frequency increases. As a result, the peak of gentle increase indicating the driving frequency in wavelet energy coefficient distribution plot will shift to left. However, this shift movement has a slight influence on the peak of sharp increase indicating the bridge frequency in wavelet energy coefficient distribution. Study found that this sharp peak will shift to left slightly. Therefore, as it is shown in Table 2, the identified frequency of bridge increases with the increment of velocity.

The approach has been applied for a 25-m span bridge; all other problem parameters are kept the same. The first and second theoretical natural frequencies of the bridge (L=25 m) are 1.39 and 5.56 Hz, respectively. Figure 7 shows the original crossing vehicle acceleration history at velocity 2 m/s and the corresponding frequencies extracted using both wavelet-based approach and FFT approach.

Figure 7b demonstrates frequencies extracted using FFT where the spectrum is dominated by first three main frequencies. Based on the work of Yang et al. [5, 13] and González et al. [30], f_1 (=0.08 Hz) corresponds to the driving frequency of the vehicle, f_2 (=1.36 Hz) presents the first natural frequency for the bridge, f_3 (=5.60 Hz) is the second fundamental bridge frequency.

Similarly, Fig. 7c shows extracted frequencies using the presented wavelet approach. It illustrates two peaks at scale a1 (= 46.9) and a2 (=180.8), respectively, which refer to 5.33 Hz and 1.38 Hz. These frequencies show a proper agreement with the bridge frequencies. The process has been repeated for different speeds, and the results are listed in Table 3.

The results in Table 3 show that the 1st mode identified frequencies from wavelet transform approach give precise results (errors less than 2.95%). The identified frequencies of the 2nd mode are worse than the 1st mode. On the other hand, as it is shown, the identified frequencies of both 1st and 2nd increase slightly with the increment of velocity. In addition, the proposed wavelet approach shows a neat identification for the bridge frequency in most cases. This



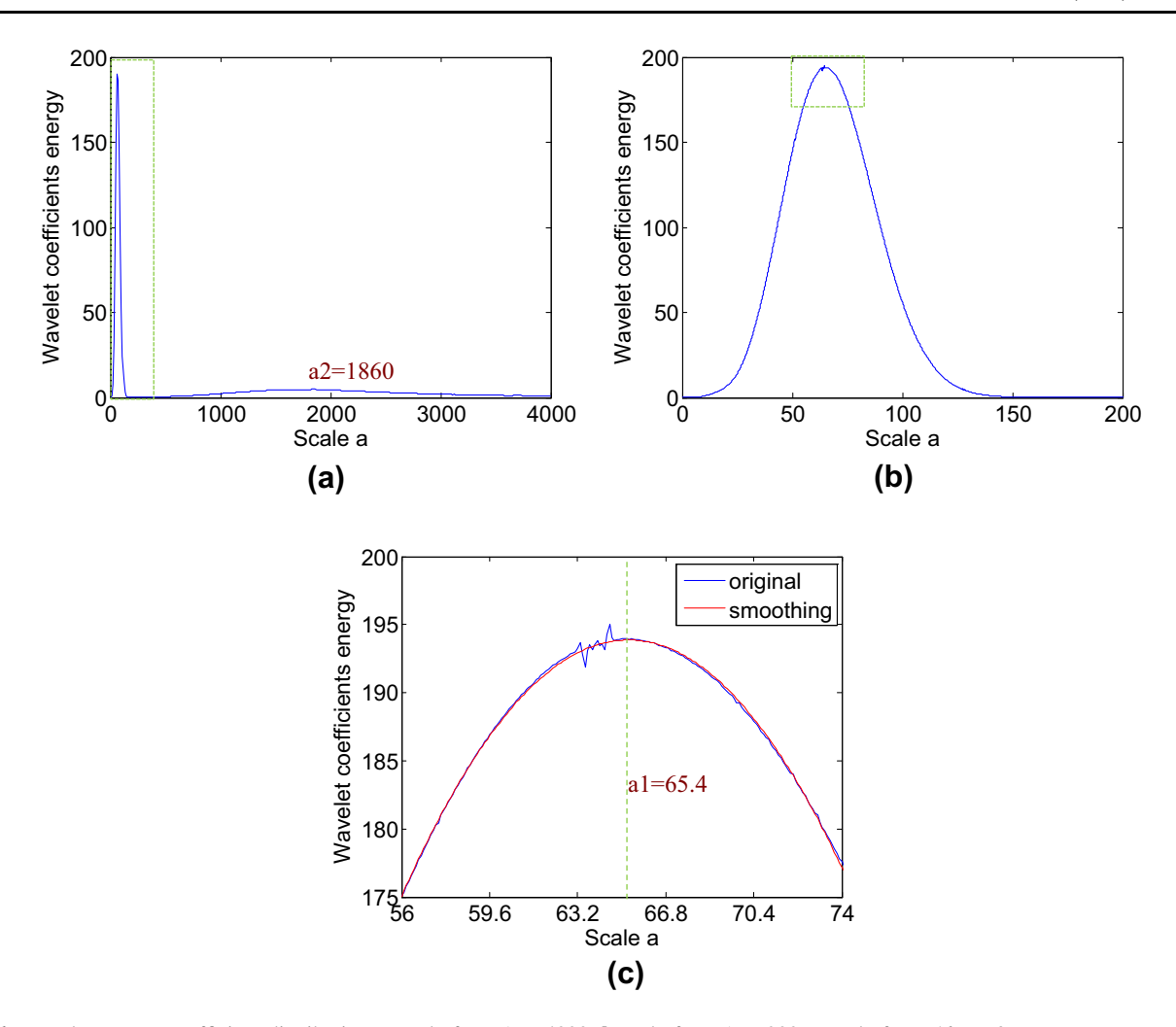


Fig. 6 Wavelet energy coefficient distribution, a scale from 1 to 4000; b scale from 1 to 200; c scale from 56 to 73

Table 2 Frequency identification at different velocities at span $L=15~\mathrm{m}$

Velocity (m/s)	Span ($L = 15 \text{ m}$) Theoretical frequency (Hz)	Frequency is calculated by wavelet transform (Hz)
2	3.86	3.82 (- 0.97%)
4		3.84 (- 0.51%)
6		3.86 (0.00%)
8		3.89 (0.88%)
10		3.91 (1.36%)

⁽⁾ presents the error between identified frequency and theoretical frequency

validates the feasibility of the proposed approach in quantifying the bridge damage as a shift in the extracted bridge frequency as it will be demonstrated in the following sections.

4 Bridge damage identification using measurements from a passing vehicle

In this section, the change in the bridge frequency is used as a damage index to quantify the damage in the bridge. Damage is modeled using Sinha et al. [31] damage model, where the damage is assumed to be extended over a region of three times the beam depth. In this affected area, the element stiffness varies from the minimum values at the crack location to full stiffness at the end of the damaged area. The level of damage is defined as ratio of the depth of the crack to the depth of the intact bridge. For example, if the damage level is 0.6 (or 60%), it means that the crack depth is 0.48 meters for a 0.8-m deep bridge.

The FFT method is due to the low frequency resolution associated with higher vehicle speeds. Therefore, and for the same reason, FFT cannot be used to monitor the bridge frequency drop due to structural damage. That the frequency step will not pick up the minor changes happened



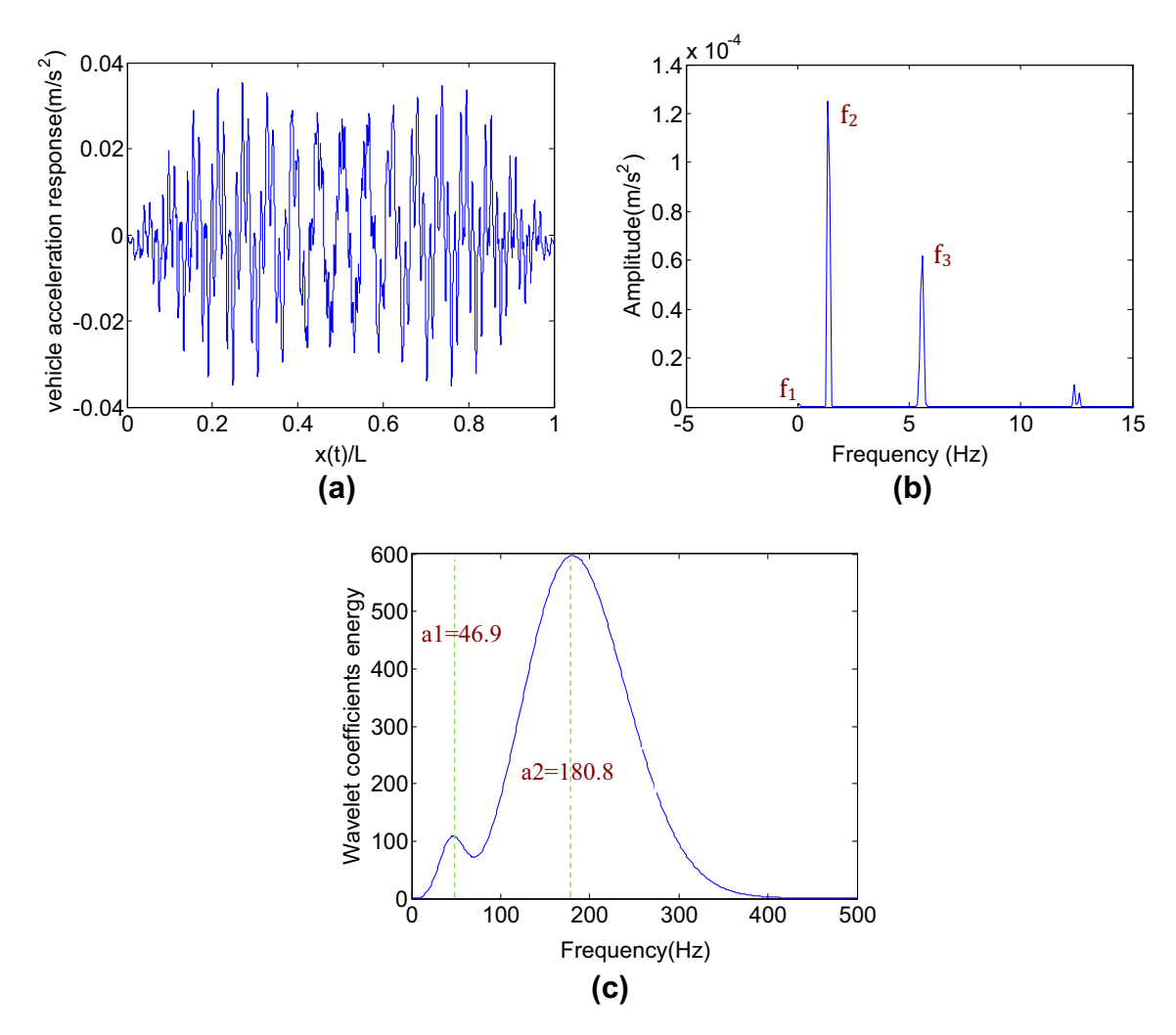


Fig. 7 a The vehicle acceleration response at span = 25 m. b Acceleration spectrum. c Wavelet coefficient energy distribution at each scale

Table 3 Frequency identification at different velocities at span L = 25 m

Velocity (m/s)	Span $(L = 25 \text{ m})$ Theoretical frequency (Hz)	Frequencies are calculated by wavelet transform (Hz)	
		1st	2nd
2	1st = 1.39	1.38 (- 0.52%)	5.33 (- 4.13%)
4	2nd = 5.56	1.39 (0.00%)	5.34 (- 3.92%)
6		1.41 (1.10%)	5.35 (- 3.72%)
8		1.42 (2.16%)	5.41 (- 2.68%)
10		1.43 (2.95%)	5.45 (- 2.04%)

() presents the error between identified frequency and theoretical frequency

to the bridge frequency due to structural damage. Therefore, the next section will focus on using the Wavelet Transform to track the change in the bridge frequency due the existence of structural damage.

Figure 8 shows the identified frequencies using wavelet analysis approach for different velocities. The damage located at the middle of the bridge. The bridge is modeled four times, one as an intact bridge, and other three cases of

different damage levels (e.g. 20, 40 and 60%). As it is shown, with the increment of damage level, the theoretical frequencies of bridge decrease $(f_{\rm TI} > f_{\rm TD1} > f_{\rm TD2} > f_{\rm TD3})$. At the same time, the identified frequencies of damaged bridge decrease as well $(f_{\rm II} > f_{\rm ID1} > f_{\rm ID2} > f_{\rm ID3})$. In this figure, the identified results and their theoretical ones matched very well (errors less than 1.36%). It is worth to notice that the identified results at the different damage



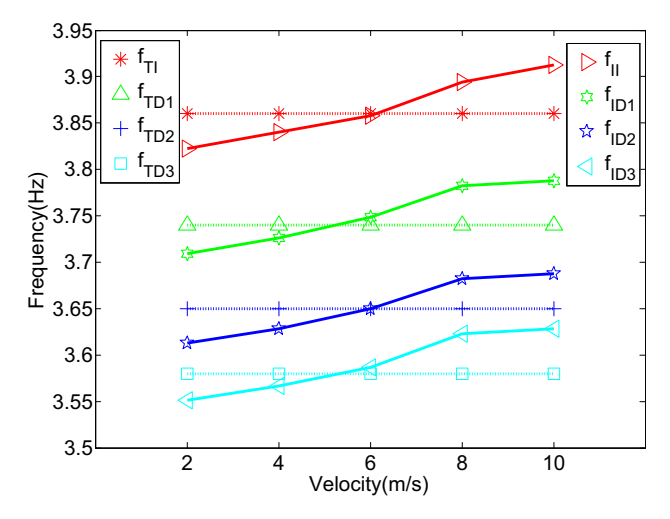


Fig. 8 Frequency identification of bridge at different velocities with wavelet analysis. $f_{\rm TI}$ presents the 1st theoretical frequency of the intact bridge, $f_{\rm TD1}$ presents the 1st theoretical frequency of the damaged bridge at level 0.2, $f_{\rm TD2}$ presents the 1st theoretical frequency of the damaged bridge at level 0.4, $f_{\rm TD3}$ presents the 1st theoretical frequency of the damaged bridge at level 0.6, $f_{\rm II}$ presents the 1st identified frequency of the intact bridge, $f_{\rm ID1}$ presents the 1st identified frequency of the damaged bridge at level 0.2, $f_{\rm ID2}$ presents the 1st identified frequency of the damaged bridge at level 0.4, $f_{\rm ID3}$ presents the 1st identified frequency of the damaged bridge at level 0.4, $f_{\rm ID3}$ presents the 1st identified frequency of the damaged bridge at level 0.6

levels are parallel to that at with intact bridge. In other words, the driving frequency will have the same effect on intact bridge or damaged bridge. That means that the identified drop frequency of bridge is very close to the theoretical one. These identified drop frequency indicates the damage exist and can be used to quantify the structural integrity of the bridge.

The same process has been repeated for the 25-m bridge. The damage is set at 0.4 L with damage level 0.2 and 0.5 respectively. The first two natural frequency of bridge is extracted for different vehicle speeds, and the results are illustrated in Figs. 9 and 10 respectively. As it is shown, the 1st frequency drop due to the structural damage is very slight $(f_{TI}-f_{TD1}=0.02 \text{ Hz}; f_{TD1}-f_{TD2}=0.02 \text{ Hz})$. Compared to the 1st frequency, the 2nd frequency showed to be more sensitive to bridge damage.

From the Figs. 9 and 10, it is obvious that the identified frequencies of the 2nd mode is worse than the 1st mode. The errors between identified result and theoretical one are less than 4.33% in Fig. 9, while errors in Fig. 10 are less than 7.73%. Similarly, the driving frequency will influence the identified results. However, as it is shown, it also shows the same effect on the intact and damaged bridge.

In summary, the identified frequency of bridge shows a drop in its magnitude due to structural damage. Even though there might be a great error between the extracted and the exact frequencies. Therefore, the proposed approach can be

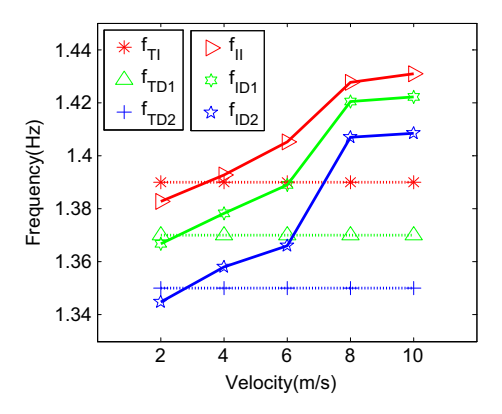


Fig. 9 1st natural frequency of bridge identification with wavelet analysis. $f_{\rm TI}$ presents the 1st theoretical frequency of intact bridge, $f_{\rm TD1}$ presents the 1st theoretical frequency of damaged bridge at level 0.2, $f_{\rm TD2}$ presents the 1st theoretical frequency of damaged bridge at level 0.5, $f_{\rm II}$ presents the 1st identified frequency of intact bridge, $f_{\rm ID1}$ presents the 1st identified frequency of damaged bridge at level 0.2, $f_{\rm ID2}$ presents the 1st identified frequency of damaged bridge at level 0.5

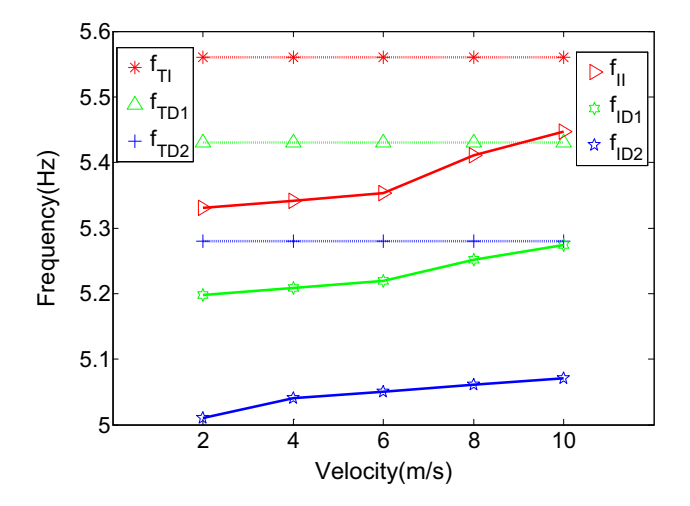


Fig. 10 2nd natural frequency of bridge identification with wavelet analysis. $f_{\rm TI}$ presents the 2nd theoretical frequency of intact bridge, $f_{\rm TD1}$ presents the 2nd theoretical frequency of damaged bridge at level 0.2, $f_{\rm TD2}$ presents the 2nd theoretical frequency of damaged bridge at level 0.5, $f_{\rm II}$ presents the 2nd identified frequency of intact bridge, $f_{\rm ID1}$ presents the 2nd identified frequency of damaged bridge at level 0.2, $f_{\rm ID2}$ presents the 2nd identified frequency of damaged bridge at level 0.5, $f_{\rm ID2}$ presents the 2nd identified frequency of damaged bridge at level 0.5.

used to quantify the existence of damage 'Level I SHM' using indirect measurements from an inspection truck.

5 Extracting bridge frequency using a half-car model

In this part, a theoretical half-car model is adopted to represent the behavior of the inspection vehicle as shown in Fig. 11. This model has four degrees of freedom



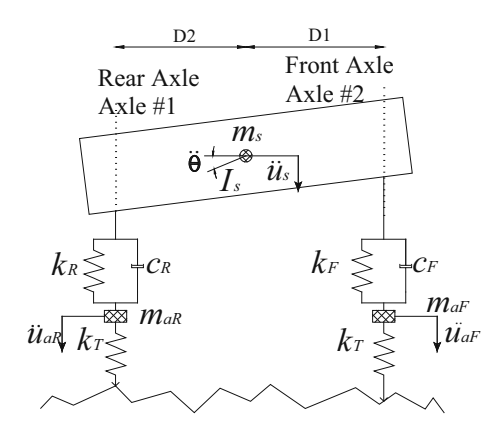


Fig. 11 Half-car model

Table 4 Parameters of half-vehicle model

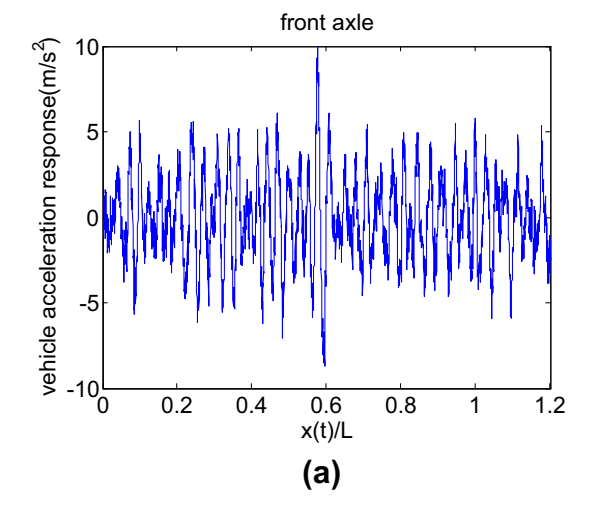
Vehicle properties			
$m_{ m s}$	16,600 kg	I_{s}	95,765 kg m ²
$k_{\mathbf{R}}$	400 kN/m	$k_{ m F}$	400 kN/m
$c_{\mathbf{R}}$	8 kN s/m	$c_{ m F}$	8 kN s/m
m_{aR}	700 kg	$m_{ m aF}$	700 kg
k_{T}	1750 kN/m	$k_{ m F}$	1750 kN/m
D2	1.05 m	D1	1.95 m

correspond to the vehicle body bouncing, u_s , the body pitch rotation, θ , and two axle mass bouncing, u_{aR} , u_{aF} . The vehicle body mass is represented by the sprung mass, m_s and its moment of inertia is represented as, I_s . The vehicle body is connected to axles through a combination of linear springs have stiffness of k_R or k_F and viscous dampers with damping coefficient, C_R or C_F . The vehicle axles have m_{aR} and m_{aF} masses, the axle masses are connected to the

ground with a springs have $k_{\rm T}$ stiffness. D1 and D2 represent the distance of each axle to the center of gravity of the vehicle. The vehicle properties are listed in Table 4. The first two vibration frequencies of the vehicle are 0.61, 1.02, 8.80 and 8.84 Hz.

In this part, the road has a roughness class 'A' defined using ISO-8608 [32]. Due to the presence of the road roughness in the problem, the profile excites the vehicle more than the bridge do and hence the vehicle frequencies domain the frequency spectrum. Neither wavelet nor FFT could obtain accuracy result for the bridge frequency. To reduce the road roughness effect, the concept of subtracting the axle acceleration signal is adopted [33]. Herein the acceleration of the rear axle is subtracted from the acceleration of the front axle after shifting the rear axle signal with an interval equal to the time spent by the rear axle to reach the front axle position. Before processing the concept of subtracting, each collected axle acceleration response is added noisy signal. The subtracted signal is then processed using the wavelet approach presented in this paper. When the velocity is 2 m/s, the front and rear axle signals added with 90 dB noisy signal are presented in Fig. 12 while the subtracted signal is shown in Fig. 13a. The introduced wavelet procedure is applied to the subtracted signal, the wavelet energy coefficient is illustrated in Fig. 13b.

Similar to the quarter-car model, a clear sharp peak is observed at scale of a1 = 65.5 and the corresponding frequency is 3.82 Hz. Another gentle peak is observed at scale a2 = 405.0 corresponding to frequency of 0.62 Hz, which is represented by the first frequency of vehicle. Noisy signal effect on this subtracting concept has been investigated and the results are listed in Table 5. As it is shown, until intensity of noisy signal to be 20 dB, the



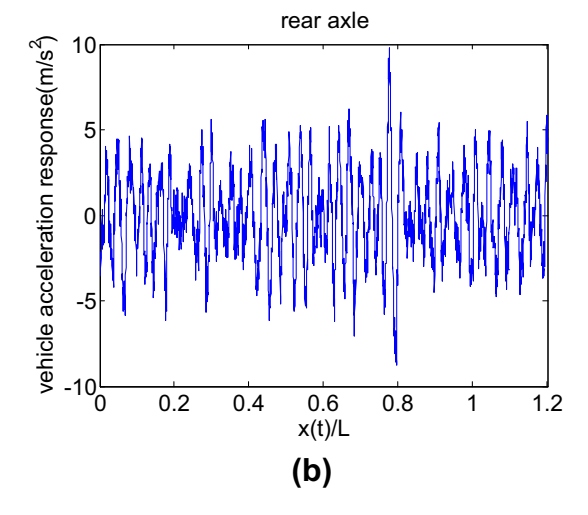


Fig. 12 a Front axle acceleration response. b Rear axle acceleration response

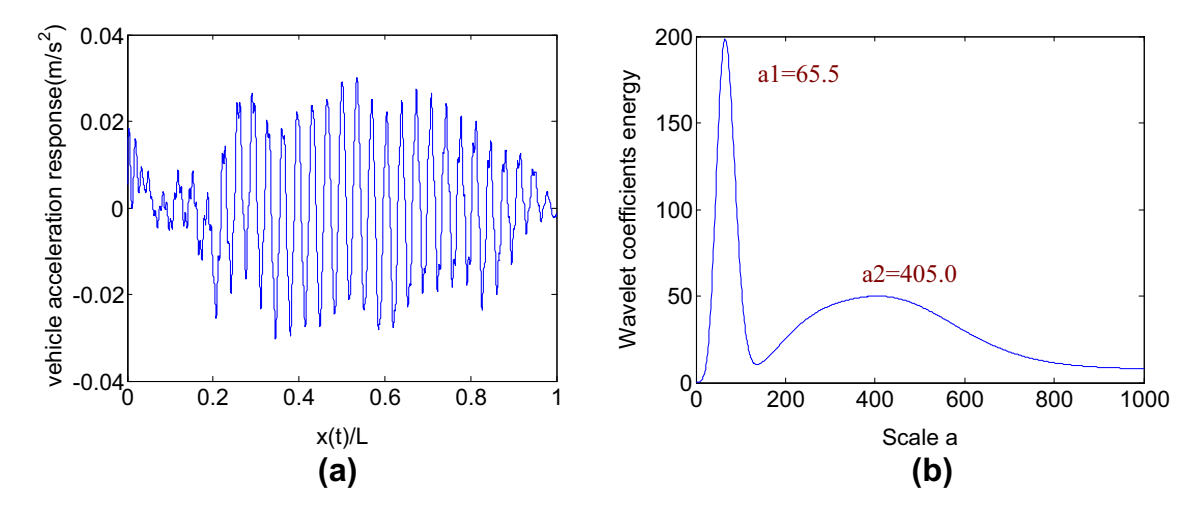


Fig. 13 a Difference of responses from two axles; b its wavelet coefficient energy distribution of each scale

Table 5 Frequency identification at different intensities of noisy signal

Intensity of noisy signal	Span ($L = 15 \text{ m}$) Theoretical frequency (Hz)	Frequency is calculated by wavelet transform (Hz)
dB 80	3.86	3.82 (- 1.03%)
dB 70		3.82 (- 1.03%)
dB 60		3.82 (- 1.03%)
dB 50		3.82 (- 1.03%)
dB 40		3.82 (- 1.03%)
dB 30		3.82 (- 1.03%)
dB 20		3.31 (- 14.19%)

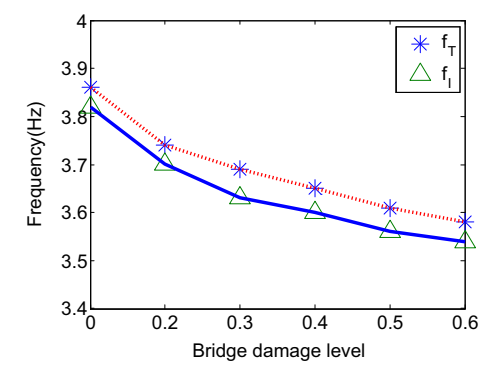


Fig. 14 Bridge frequency identification at different damage levels with velocity of 2 m/s. f_T presents the theoretical frequency of intact bridge or damaged bridge, f_I presents the identified frequency of intact bridge or damaged bridge; damage level 0 means intact bridge

difference response with wavelet transform shows a precise identified frequency of bridge.

Although road roughness is one of main challenges in "drive-by" monitoring system, the concept of subtracting signals from identical axles is an effective way to decrease its effect or even remove it. Here Fig. 14 shows the identified frequencies of the bridge for different damage levels

for a velocity of 2 m/s considering the intensity of noisy signal at 40 dB, comparing to their corresponding theoretical frequencies. In this case, the damage is simulated at mid-span. As it is shown, the identified frequencies of bridge are very close to their theoretical frequencies (errors less than -1.53%). In addition, with the increment of damage level, both of identified frequency and theoretical frequencies decrease.

6 Conclusions

This paper introduces a new method to extract the natural frequency of bridge from indirect measurements of a passing vehicle, based on wavelet analysis. In compare with FFT, the proposed approach is not restricted to the frequency resolution. The approach has been extended to point out to the frequency drop due to the structural damage. The extracted bridge frequencies using the proposed wavelet approach show a drop in its magnitude as the damage extent increases. However, the value of the extracted frequency did not show a good agreement with the theoretical bridge frequency. In contrast, FFT did not



show any evidence for damage in the acceleration spectrum. The same results have been found for higher modes of vibrations (2nd mode). The paper examined the sensitivity of the proposed approach to road roughness profile. In this regard, a Half-Car model with two axles has been utilized, and the signal of the axles have been subtracted with time lag to damp out the road roughness effect on the recorded signal. The subtracted acceleration has been processed using the proposed method and the results shows good agreement between the extracted and theoretical bridge frequencies. The approach has strong potential to provide a quick estimation for the bridge health condition.

Acknowledgements This research is sponsored by National Science of Foundation (NSF-CNS-1645863). Any opinions, findings, and conclusions or recommendations expressed in this publication are those of the authors and do not necessarily reflect the view of the sponsors.

References

- Malekjafarian A, McGetrick PJ, Obrien EJ (2015) A review of indirect bridge monitoring using passing vehicles. Shock Vib 2015:1–16
- Chupanit P, Phromsorn C (2012) The importance of bridge health monitoring. Int Sci Index 6:135–138
- Rytter A (1993) Vibrational based inspection of civil engineering structures. PhD diss., Dept. of Building Technology and Structural Engineering, Aalborg University
- Carden EP, Fanning P (2004) Vibration based condition monitoring: a review. Struct health Monit 3(4):355–377
- Yang YB, Lin CW, Yau JD (2004) Extracting bridge frequencies from the dynamic response of a passing vehicle. J Sound Vib 272(3-5):471-493
- Yang YB, Lin CW (2005) Vehicle-bridge interaction dynamics and potential applications. J Sound Vib 284(1):205–226
- Yang YB, Chang KC (2009) Extraction of bridge frequencies from the dynamic response of a passing vehicle enhanced by the EMD technique. J Sound Vib 322(4–5):718–739
- Lin CW, Yang YB (2005) Use of a passing vehicle to scan the fundamental bridge frequencies: an experimental verification. Eng Struct 27(13):1865–1878
- Yang YB, Li YC, Chang KC (2014) Constructing the mode shapes of a bridge from a passing vehicle: a theoretical study. Smart Structures and Systems 13(5):797–819
- González A, O'Brien EJ, McGetrick P (2010) Detection of bridge dynamic parameters using an instrumented vehicle. In: 5th world conference on structural control and monitoring, Tokyo, Japan, 12–14 July
- Yang YB, Chang KC (2009) Extracting the bridge frequencies indirectly from a passing vehicle: parametric study. Eng Struct 31(10):2448–2459
- Siringoringo DM, Fujino Y (2012) Estimating bridge fundamental frequency from vibration response of instrumented passing vehicle: analytical and experimental study. Adv Struct Eng 15(3):417–433
- Yang YB, Chang KC, Li YC (2013) Filtering techniques for extracting bridge frequencies from a test vehicle moving over the bridge. Eng Struct 48:353–362

- McGetrick P, Hester D, Taylor S (2017) Implementation of a drive-by monitoring system for transport infrastructure utilising smartphone technology and GNSS. J Civil Struct Health Monit 7(2):175–189
- OBrien EJ, Martinez D, Malekjafarian A, Sevillano E (2017)
 Damage detection using curvatures obtained from vehicle measurements. J Civil Struct Health Monit 7(3):333–341
- Fujino Y, Kitagawa K, Furukawa T, Ishii H (2005) Development of vehicle intelligent monitoring system (VIMS). In: Tomizuka M (ed) Proceedings of SPIE - the international society for optical engineering, vol 5765, 1st edn. San Diego, CA, pp 148–157
- Khorram A, Bakhtiari-Nejad F, Rezaeian M (2012) Comparison studies between two wavelet based crack detection methods of a beam subjected to a moving load. Int J Eng Sci 51:204–215
- Poudel UP, Fu G, Ye J (2007) Wavelet transformation of mode shape difference function for structural damage location identification. Earthquake Eng Struct Dyn 36(8):1089–1107
- Shahsavari V, Bastien J, Chouinard L, Clément A (2017) Likelihood-based testing of wavelet coefficients for damage detection in beam structures. J Civil Struct Health Monit 7(1):79–98
- Nguyen KV, Tran HT (2010) Multi-cracks detection of a beamlike structure based on the on-vehicle vibration signal and wavelet analysis. J Sound Vib 329(21):4455–4465
- McGetrick PJ, Kim CW (2013) A parametric study of a drive by bridge inspection system based on the Morlet wavelet. Key Eng Mater 569–570:262–269
- Khorrami H, Moavenian M (2010) A comparative study of DWT, CWT and DCT transformations in ECG arrhythmias classification. Expert Syst Appl 37(8):5751–5757
- Morley J, Arens G, Fourgeau I, Giard D (1982) Wave propagation and sampling theory: part I. Geophysics 47:203–221
- Morlet J (1983) Sampling theory and wave propagation. Springer, Berlin
- Gao RX, Yan R (2011) Selection of base wavelet. Springer, Berlin
- Cebon D (1999) Handbook of vehicle-road interaction. Swets & Zeitlinger, Netherlands
- Harris NK, OBrien EJ, González A (2007) Reduction of bridge dynamic amplification through adjustment of vehicle suspension damping. J Sound Vib 302(3):471–485
- Elhattab A, Uddin N, OBrie E (2016) Drive-by bridge damage monitoring using bridge displacement profile difference. J Civil Struct Health Monit 6(5):839–850
- Elhattab A, Uddin, N, Obrien E (2015) Drive-by bridge damage detection using apparent profile. In: first international conference on advances in Civil Infrastructure And Construction Materials (CISM), pp 33–45
- 30. González A, Covián E, Madera J (2008) Determination of bridge natural frequencies using a moving vehicle instrumented with accelerometers and GPS. In: Proceedings of the 9th international conference on computational structures technology, Civil-Comp Press, Athens, Greece, 2–5 September
- Sinha JK, Friswell MI, Edwards S (2002) Simplified models for the location of cracks in beam structures using measured vibration data. J Sound Vib 251(1):13–38
- ISO-8608 (1995) Mechanical vibration-Road surface profiles-Reporting of measured data. International Organization for Standardization (ISO), Geneva, Geneva
- Keenahan J, Brien EJ, McGetrick PJ, González A (2013) The use of a dynamic truck-trailer drive-by system to monitor bridge damping. Struct Health Monit 13:143–157 (1475921713513974)

